Research article

Declining tree growth rates despite increasing water-use efficiency under elevated CO_2 reveals a possible global overestimation of CO_2 fertilization effect
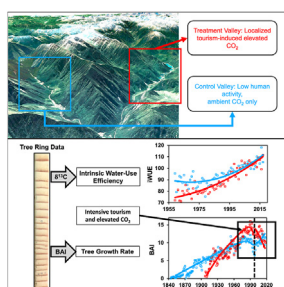
Benjamin Laffitte [a], Barnabas C. Seyler [a], Wenzhi Wang [b], Pengbo Li [a], Jie Du [c], Ya Tang [a,*]

[a] Department of Environment, College of Architecture and Environment, Sichuan University, No. 24, South Section One, First Ring Road, Chengdu, Sichuan 610065, China
[b] The Key Laboratory of Mountain Environment Evolution and Regulation, Institute of Mountain Hazards and Environment, Chinese Academy of Sciences, Chengdu, Sichuan 610041, China
[c] Jiuzhaigou Administrative Bureau, Zhangzha, Jiuzhaigou, Sichuan 623402, China

GRAPHICAL ABSTRACT

ARTICLE INFO

ABSTRACT

Though rising atmospheric CO_2 concentrations (C_a) harm the environment and society, they may also raise photosynthetic rates and enhance intrinsic water-use efficiency (iWUE). Numerous short-term studies have investigated tree growth under elevated CO_2 (eCO_2) conditions, but no long-duration study has investigated eCO_2 impacts on tree growth and iWUE under natural conditions. Utilizing a new dendrochronological experimental design in a heavily-touristed nature preserve in Southwest China (Jiuzhaigou National Nature Reserve), we compared tree growth (e.g., basal area increment) and iWUE in two biophysically and environmentally similar valleys with contrasting anthropogenic activities. Trees in the control valley with ambient CO_2 benefited from increasing C_a, possibly due to the CO_2 fertilization effect and optimal environmental conditions. However, trees in the treatment valley with intensive tourism experienced comparatively higher localized eCO_2 and growth rate declines. While iWUE increased (1959–2017) in the control (25.3%) and treatment sites (47.8%), declining tree growth rates in the treatment site was likely because comparatively extreme CO_2 exposure levels encouraged stomatal closures. As the first long-term study investigating eCO_2 impacts on tree growth and iWUE under natural conditions, we demonstrate that increased forest iWUE is unlikely to overcome negative drought stress and rising temperature impacts. Thus, forest potential for mitigating eCO_2 and global climate change is likely overestimated, particularly under dry temperate conditions.

* Corresponding author.
E-mail address: tangya@scu.edu.cn (Y. Tang).

1. Introduction

Atmospheric CO_2 concentrations (C_a) from anthropogenic emissions have been steadily increasing from approximately 280 ppm before the Industrial Revolution (1750s) to 385 ppm in 2009, and approximately 410 ppm in 2019 (US Department of Commerce, 2019). Current projections predict concentrations will reach 500–1,000 ppm by 2100 (Hayhoe et al., 2017; Nordhaus, 2018). Removing CO_2 from the atmosphere is one of the most important challenges to avoid significant increases in temperatures, minimize ecosystem degradation, and minimize other detrimental environmental and social consequences (Huntingford and Oliver, 2021). Active carbon removal methods can take numerous forms, from new technologies to land management practices, but they have been mostly used on a small scale because of their costly designs (Hepburn et al., 2019). However, trees have a strong innate potential to remove atmospheric CO_2 and are naturally cost effective (Lewis et al., 2019). Nevertheless, how trees respond to increasing CO_2 and estimates of how much CO_2 can be stored by forests on a global scale remain unclear because they depend on so many factors, including how these may differ between biomes (Wang et al., 2020).

Studying the impact of elevated CO_2 (eCO_2) on forest ecosystems is one of the biggest challenges in forest ecology and climate change research because of its importance for the global carbon cycle and its consequences for future climate (Bonan, 2008; Zhu et al., 2016). That eCO_2 increases the photosynthesis rate in C_3 plants and, therefore, the growth of trees has also sometimes been documented, hence the CO_2 fertilization effect (CFE) (Kimball, 1983; Acock and Allen, 1985; Cure and Acock, 1986; Allen et al., 1994; Rozema, 1993; Allen, 1994; Allen and Amthor, 1995). Other studies have found limited (Gedalof and Berg, 2010) to no CFE (Tognetti et al., 2000). Nevertheless, as an application of the CFE hypothesis, tree radial growth tends to increase along with increasing C_a. Over the past 30 years, CO_2 enrichment experiments like Free-air CO_2 enrichment (FACE) (Hendrey et al., 1993; Grant et al., 1995; Ainsworth and Long, 2005; Norby and Zak, 2011) and open-top chamber experiments (Drake et al., 1989; Dore et al., 2003; Bishop et al., 2014) have widely found evidence supporting the CFE hypothesis. However, these approaches have been criticized mainly for two reasons. First, the short, high-concentration bursts of CO_2 used in these experiments do not represent the more slowly rising CO_2 levels under natural conditions (Wang et al., 2006). Second, the average duration of these experiments is only four years (Jones et al., 2014) and short-term CFE experiments are unreliable for drawing conclusions about long-term tree growth (Walker et al., 2021).

Unlike CO_2 enrichment experiments, tree ring studies (dendrochronology) can provide important, long-term information about tree growth under natural conditions (Fritts, 1976). Nevertheless, dendrochronological methods are much less commonly used when investigating the CFE, and they have shown mixed results (Schweingruber et al., 1993; Mieli-Kainen and Timonen, 1996; Gedalof and Berg, 2010; Girardin et al., 2011, 2016; Bader et al., 2013; van der Sleen et al., 2014). Indeed, due to the possibly confounding impacts of climate change, nitrogen deposition, and increasing CO_2, it is necessary to carefully choose study site locations and target species to isolate the effects of CO_2 (Wang et al., 2006; Brienen et al., 2012). Only two studies have used CO_2 springs (~1,500 ppmv), allowing direct comparison of two nearby sites with similar climatic conditions and soil properties for long-term tree growth analysis (Hattenschwiler et al., 1997; Tognetti et al., 2000). Hattenschwiler et al. (1997) found trees benefited from elevated CO_2 under drought stress, but Tognetti et al. (2000) showed that tree growth at the CO_2-enriched site was not significantly different from growth at the control site.

In a global change context, long-term tree physiology variations using stable carbon isotopes ($\delta^{13}C$) have been extensively investigated (Gómez-Guerrero et al., 2013; Tognetti et al., 2014; van der Sleen et al., 2014; Maxwell et al., 2019). By studying the compositions in tree-ring $\delta^{13}C$, it is possible to calculate the intrinsic water-use efficiency (iWUE). Defined as the ratio of net photosynthesis fluxes (A) to water

vapor conductance (g_w), iWUE indicates the cost of assimilation per unit of water, expressed in micromole per mol ($\mu mol\ mol^{-1}$) (Ehleringer and Cerling, 1995). Stomata tend to close under eCO_2 for plants to save water, often resulting in improved iWUE (Farquhar et al., 1989; Nock et al., 2011; Guerrieri et al., 2019). Thus, the iWUE is an important component of water-carbon coupling and process management in terrestrial ecosystems (Osmond et al., 1980). Many iWUE studies have been conducted in temperate (Feng, 1999; Waterhouse et al., 2004; Saurer et al., 2014; Frank et al., 2015), boreal (Saurer et al., 2004; Silva et al., 2010; Gagen et al., 2011; Peñuelas et al., 2011), and tropical forest ecosystems (Hietz et al., 2005; Brienen et al., 2011; van der Sleen et al., 2014; Li et al., 2017). Despite consistent results showing increased iWUE across biomes and species, the mechanisms involved in forest adaptation to climate change remain uncertain. Many studies have found declining growth even with increasing iWUE (Andreu-Hayles et al., 2011; Peñuelas et al., 2011; Lévesque et al., 2014; van der Sleen et al., 2014; Xu et al., 2018). Furthermore, manipulative experiments (e.g., FACE experiments, open-top chambers) have provided valuable insights into temperate forest growth dynamics under eCO_2 (Rahman et al., 2019), but no study has yet been conducted under natural conditions over a sufficiently-long duration. Hence, it is crucial to explore variations in tree growth along with stable carbon isotopes and iWUE under natural conditions and eCO_2 (Walker et al., 2021; Way et al., 2021).

In this study, we propose a new experimental design using a dendrochronological approach within a nature preserve. In it, trees were sampled from two neighboring valleys with similar climate conditions but different anthropogenic activities in Southwest China's Jiuzhaigou National Nature Reserve (JNR). Within JNR, tourism first began in 1984 (with just 27,529 visitors) and was characterized by a relatively slow growth rate until 1997 (183,148 visitors) (Zhang et al., 2021). The period from 1998 to 2007 was characterized by fast growth reaching more than 2.5 million (2007). After the 2008 Wenchuan Earthquake-induced decline in 2008, the subsequent period was characterized by very rapid growth until reaching a peak of five million per year in 2015 and 2016 (Qiao et al., 2018; Zhang et al., 2021) (Figure S1). Consequently, localized atmospheric CO_2 increased where tourist activities intensified, peaking in certain locations at more than 800 ppm during tourist seasons (e.g., in one but not the other valley). Our objectives were to: (1) determine how tree growth is affected by different concentrations of localized anthropogenically-induced eCO_2, (2) assess long-term tree growth and iWUE variations in response to eCO_2, and (3) understand the long-term relationship between climate, tree growth, and iWUE under eCO_2, to better predict the future potential of forests at mitigating atmospheric CO_2. Assuming the CFE to be correct, we hypothesized that localized eCO_2 concentrations induced by human activities will lead to improved tree growth rate (through the CFE) and iWUE.

2. Materials and method

2.1. Study area

JNR (32°55′–33°16′N and 103°46′–104°05′E) lies on the southeast edge of the Qinghai-Tibet Plateau in the transitional area between the humid, subtropical Sichuan Basin and the semi-arid, cold highlands (Figure 1A) (Du et al., 2018). Covering a watershed of 640 km^2, with elevations between 1,996 and 4,789 m above sea level (asl), JNR is surrounded by the peaks of the Min Mountain Range. Famous for its spectacularly colorful lakes, waterfalls, and rivers (Figure 2), JNR is listed as World Heritage Site by UNESCO and is one of the most visited tourist destinations in China.

2.2. Climate data

Because of its high elevation, dramatic altitudinal gradient, and monsoon impacts, JNR's climate is temperate, characterized by distinct dry and wet seasons (Figure 3). There were only 19 years of JNR

meteorological data (first recorded in 2000) at the time of correlation analysis (2018). However, Songpan Meteorological Station, the next closest station to JNR (China Meteorological Data Service Centre), has recorded meteorological data since 1951. High correlation between the two sites justified using the Songpan meteorological data for this study (Figure S2), which spanned 69 years (1951–2019; Figure S3).

2.3. Sampling strategy

In the present study, we used JNR's unique field conditions to examine how anthropogenically-induced eCO_2 on the local scale may affect tree growth by comparing two nearby sites (Zharu and Shuzheng valleys) with the same climatic conditions but different human activities (Figures 2A and 2B). Zharu Valley has not been strongly impacted by heavy tourism in JNR because its scenery is not as spectacular as Shuzheng, Rize, and Zezhawa valleys. Despite the presence of a temple located near its entrance, CO_2 induced by tourism and other human activities remain negligible. Therefore, we chose Zharu Valley as the "control" site (control valley).

In contrast to Zharu, Shuzheng Valley, along with Rize and Zezhawa valleys (Figures 2C and 2D), is heavily visited by tourists. Due to its position at the confluence of Rize and Zezhawa valleys, Shuzheng valley receives all vehicles and tourists passing through the park. Consequently, localized CO_2 emissions in Shuzheng can be very high, especially during peak tourist seasons (April to November; Figure 4 and Table 1). Although the concentration of CO_2 does mix rapidly and does not greatly vary spatially on the global scale, it does matter at the local scale, where topography and micro-climate contributes to significant variability at emission sources (Wang et al., 2007). As a highly vegetated valley with steep-slopes, diffusion of tourism-origin CO_2 at the valley floor is much slower than in an open environment. Therefore, we chose Shuzheng Valley as the "treatment" site (treatment valley) (Figure 1B).

Based on our preliminary investigations and the results of previous studies on the ecology and vegetation distribution of pine forests in JNR (Liu et al., 2007), we selected *Pinus tabuliformis* Carrière (Chinese pine) as the target species. Being native to the area, Chinese pine forms forests largely distributed below an elevation of 2,700 m. In both treatment and control valleys, we sampled against the slope along an altitudinal gradient at 00 m (road level), 10 m, 20 m, 30 m, 50 m, and 70 m with three replicates per valley (Figure 1C). Since the understanding of CO_2 dispersion in JNR was still unknown, this design could provide insight concerning the CO_2 effect on trees at different elevations above the road. Depending on abundance and availability, two to four mature, healthy trees were sampled at each elevation. Two perpendicular cores were taken from the trunk of each tree at breast height (1.3 m) using a 5.15 mm increment borer. A total of 100 and 94 cores were collected in the treatment and the control valley, respectively.

It is well known that soil moisture influences tree growth (Veihmeyer and Hendrickson, 1950; Bassett, 1964). Also, the structure of tree rings may vary depending on the slope at ground level (Fritts, 1976). Slope and soil moisture data were therefore collected to ensure minimal differences between both valleys (Figure S4). While some differences were found between replicates (soil moisture: $p = 0.00362$; slope: $p = 9.066e^{-06}$), our results showed that there were no significant differences in soil moisture (Kruskal-Wallis test, $p = 0.2163$) or slope between valleys (Kruskal-Wallis test, $p = 0.3296$).
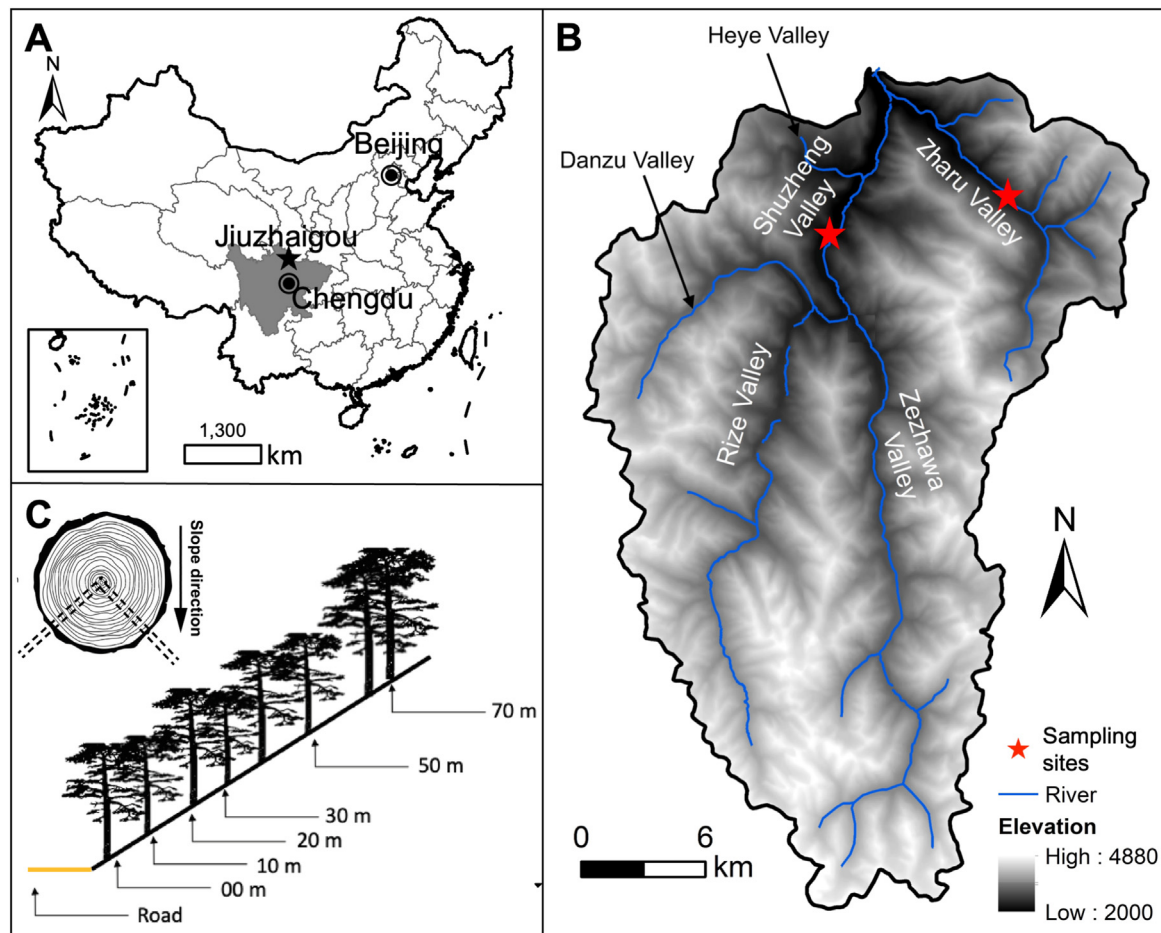

Figure 1. Jiuzhaigou National Nature Reserve geographical location (**A**), sampling sites (**B**), and sampling strategy with tree core sampling direction (**C**).

2.4. Tree growth analysis

The collected increment cores were treated by standard dendrochronological procedures. Cores were first air dried for a week, mounted in wooden core mounts, and then sanded using 400 to 1600 grit sandpaper. The tree-ring widths were measured (0.01 mm resolution) using the Lintab-6 platform (RinnTech, Heidelberg, Germany) supported by TSAP-Win software (Rinn, 2003). Cross-dating was checked according to the Gleichläufigkeit (GLK-coefficient of coherence between two chronologies), Student T-value, and Cross Date Index (CDI). Important statistics were calculated to better describe the chronologies for the study area (Table 2).

High series intercorrelation and average mean sensitivity indicated successful cross-dating. Expressed population signal (EPS) values met signal strength acceptance for the full period covered by tree-ring data. The values being largely above the threshold of 0.85 indicated a good quality and a strong signal in the records (Table 2) (Wigley et al., 1984). Also, the average core series length in the control valley (105.7 years) was longer than in the treatment valley (70.8 years). Results from a correlation matrix in the control valley showed no significant differences in basal area increment (BAI, a proxy for tree growth rate) variation between the different altitudes above the road (Figure S5A), with similar results found in the treatment valley (Figure S5B). Therefore, the BAI chronology was calculated for all 47 trees in the control valley and 50 trees in the treatment valley.

Standard detrending processes (e.g., negative exponential, linear regression, or spline) commonly used in dendroclimatology can eliminate high and/or low frequency variations in tree-ring time series (Cherubini et al., 1998; Tognetti et al., 2000; D'Arrigo et al., 2008). Thus, BAI is a more accurate proxy for tree growth in studies utilizing climate
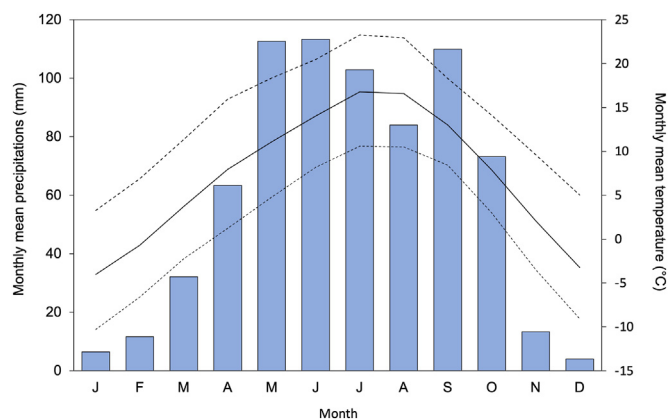

Figure 3. Regional climate summary in JNR. The mean minimum temperature is represented by the lower dotted line. The mean maximum temperature is represented by the upper dotted line. The mean temperature is represented by the black line. Data were provided by Nuorilang weather Station, from 2000 to 2018).

data because long-term biological growth trends are unaffected by detrending techniques (Rubino and McCarthyz 2004; Biondi and Qeadan, 2008; Silva and Anand, 2013). BAI not only accounts for the tendency of tree growth to vary with tree age/size, but it can also fully reflect the effects of other long-term trends such as climatic factors on tree growth (Biondi and Qeadan, 2008; Cherubini et al., 2021). Ring width values (mm yr^{-1}) were converted into BAI (mm^{-2} yr^{-1}) defined as in Eq. (1):

Figure 2. Representative scenery of four main valleys in Jiuzhaigou National Nature Reserve. In (**A**) Shuzheng Valley (treatment valley) (**B**) Zharu valley (control valley) (**C**) Rize Valley, and (**D**) Zezhawa Valley. Photo Credits: Jiuzhaigou Administrative Bureau.
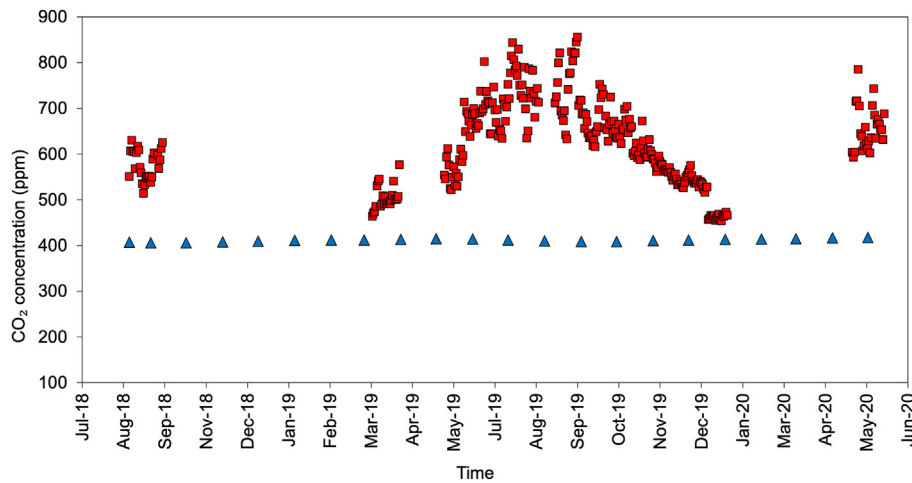
Figure 4. Atmospheric CO_2 concentrations recorded in Shuzheng Valley (August 2018–May 2020). Data were collected by our laboratory (Sichuan University). Recorded concentrations are indicated with red squares. Global ambient CO_2 levels (blue triangles) were obtained from the Mauna Loa Observatory (gml.noaa.gov/ccgg/trends/).

Table 1. CO_2 concentration from March 2019 to December 2019.

Month	Average	Min	Max
March	502	456	682
April	502	463	609
May	559	489	712
June	664	499	932
July	726	523	1011
August	729	555	957
Sept	706	558	992
October	665	552	918
November	591	538	796
December	541	498	612

$$BAI = \pi \times \left(R_n^2 - R_{n-1}^2 \right) \qquad (1)$$

where R refers to the radius at breast height of a tree in a given year and n refers to the year (Bunn, 2010; West, 1980).

2.5. Seasonality analysis

To test the relationship of seasonality and climate variables (e.g., temperature and precipitation) to tree growth, the R package "bootRes" (Zang and Biondi, 2013) was used to run bootstrapped correlations (1, 000 repetitions; Pearson's method). This method was initially described in the program DENDROCLIM 2002 (Biondi and Waikul, 2004). The functions "mdcc" from "bootRes" clones the functionality and calculates bootstrapped moving correlation functions in the same fashion (Biondi and Waikul, 2004).

2.6. Carbon isotope analysis and iWUE

In the case of stable carbon isotope analysis in dendroclimatology, direct analyses of the whole wood shavings produce ambiguous result, both temporally and chemically (Wilson and Grinsted, 1977; Burk and Stuiver, 1981). Instead, an α-cellulose extraction avoids isotope variations caused by the different relative abundances of multiple wood constituents, which generally have dissimilar isotopic signatures (Tognetti et al., 2014). For this reason, data are often derived from a single wood constituent such as the α-cellulose (Mazany et al., 1980; Marshall and Monserud, 1996). We followed a modified version of Brendel's protocol for the α-cellulose extraction (Brendel et al., 2000).

Purified tree-ring α-cellulose samples were tested for $\delta^{13}C$ analysis using Isotope Ratio Mass Spectrometry (IRMS; IsoPrime 100) coupled with an Elemental Analyser (EA; Vario PYRO Cube, Elementar Analyzen Systeme, Germany). This experiment was carried out at the Key Laboratory of Mountain Ecological Restoration and Bioresource Utilization of Sichuan Province, Chengdu Institute of Biology, the Chinese Academy of Sciences. The isotopic signature of the CO_2 produced by α-cellulose composition was measured to obtain $\delta^{13}C$ (1959–2018). The results from the isotope ratio deviations were calculated using the following common δ notation shown in Eq. (2):

$$\delta = \left(\frac{R_{sa}}{R_{re}} - 1 \right) \times 1000‰ \qquad (2)$$

where R_{sa} refers to the ratio of the ^{13}C–^{12}C isotopes in a sample and the standard reference (R_{re}). The standard deviation of the present analysis was less than 0.3‰.

Tree-ring $\delta^{13}C$ data were used to calculate carbon isotope discrimination ($\Delta^{13}C$), which is defined as the difference in isotopic values between atmospheric CO_2 ($\delta^{13}C_a$) and plant organic matter ($\delta^{13}C_p$) in ‰. $\Delta^{13}C$ is shown in Eq. (3):

Table 2. Descriptive statistics for raw ring width in Zharu (control valley) and Shuzheng (treatment valley) valleys.

Sites	Zharu Valley (control)	Shuzheng Valley (treatment)
Elevation (m)	2340–2360	2320–2370
Max. Time span	1844–2018	1907–2018
Average series length	105.7 years	70.8 years
Sampled trees	47	50
MRW	1.66	2.43
MS	0.19	0.20
SD	0.90	2.38
SI (Std Dev)	0.37 (0.20)	0.44 (0.15)
R-bar	0.31	0.56
AC1 (Std Dev)	0.84 (0.09)	0.81 (0.16)
EPS	0.93	0.98

MRW = Mean Ring Width in mm; MS = Mean Sensitivity; SD = Standard Deviation; SI = series intercorrelation; R-bar = Mean of inter-series correlations; AC1 = first order autocorrelation; EPS = Expressed population signal. For SI and AC1, Std Dev stands for Standard deviation.

$$\Delta^{13}C = \frac{\delta^{13}C_a - \delta^{13}C_p}{1 + \frac{\delta^{13}C_p}{1000}} \qquad (3)$$

where $\delta^{13}C_a$ is the $\delta^{13}C$ value of ambient air and $\delta^{13}C_p$ is the $\delta^{13}C$ value of the tree-ring α-cellulose.

For C3 plants, carbon isotope discrimination is also expressed by the following Eq. (4), according to the model proposed by Farquhar et al. (Farquhar et al., 1989), $\Delta^{13}C$ and $\delta^{13}C$ have different trends:

$$\Delta^{13}C = a + (b - a) \ \frac{C_i}{C_a} \qquad (4)$$

where a is the discrimination against $^{13}CO_2$ during CO_2 diffusion through the stomata ($a = 4.4‰$), b is the discrimination associated with carboxylation ($b = 27‰$), and C_i and C_a are the intercellular and ambient atmospheric CO_2 concentrations, respectively.

Then we determined C_i values by using Eq. (5):

$$C_i = \frac{\delta^{13}C_a - \delta^{13}C_p}{1 + \frac{\delta^{13}C_p}{1000}} - a \times \frac{C_a}{b - a} \qquad (5)$$

where $\delta^{13}C_a$ is the $\delta^{13}C$ value of ambient air and $\delta^{13}C_p$ is the $\delta^{13}C$ value of the tree-ring α-cellulose and a is the discrimination against $^{13}CO_2$ during CO_2 diffusion through the stomata ($a = 4.4‰$), b is the discrimination associated with carboxylation ($b = 27‰$), and C_i and C_a are the intercellular and ambient CO_2 concentrations, respectively. The $\delta^{13}C_a$ values were derived from ice cores (McCarroll and Loader, 2004). For data after the year 2003, a linear regression was used to interpolate the values based on measurements from Mauna Loa Observatory. C_a data were taken from direct measurements at the Mauna Loa Observatory since 1959 (US Department of Commerce, 2019).

The iWUE is expressed as the ratio of net photosynthesis (A) to stomatal conductance for water vapor (g_w) and is given by Eq. (6) (Ehler-inger and Cerling, 1995):

$$iWUE = \frac{A}{g_w} = \frac{(C_a - C_i)}{1.6} \qquad (6)$$

where the denominator of 1.6 is the ratio of gaseous diffusivities of CO_2 and water vapor in the air. Regression analyses and statistical tests were used to identify significant trends in $\delta^{13}C$, $\Delta^{13}C$, iWUE, and BAI from 1959 to 2017. We chose a 60-year time range to ensure sufficient data, and at least seven years data before widespread human activity began (the year 2018 was not included in our results to avoid any bias caused by the earthquake that occurred in August 2017), and to test the relationships between iWUE and BAI, between iWUE and environmental factors (atmospheric CO_2 concentration, annual mean temperature, and annual precipitation).

3. Results

3.1. Tree growth in the control and treatment valleys

There was a constant and strong increase in BAI from 1844 to 1997 in the control valley (Figure 5). The slope coefficient (β) from the linear regression line was 7.71 ($R^2 = 0.90$; $p < 2.2e^{-16}$, 1844 to 1997). A second linear regression was done on a subset of data from 1998 to 2017, which overlapped the periods of rapid and very rapid increase in tourist numbers to JNR after accessibility was greatly improved. During this period, the slope coefficient was higher (β = 14.03; $R^2 = 0.26$; $p = 0.02263$). In addition, there was a clear decrease in BAI between 1991 (BAI = 11.08 cm^2 year^{-1}) and 1998 (BAI = 6.55 cm^2 year^{-1}) that could be explained by extreme drought during this period (Figure S6).

In the treatment valley, BAI from 1907 to 1997 increased faster than in the control valley (β = 13.48; $R^2 = 0.85$; $p < 2.2e^{-16}$; Figure 5). In contrast to that in the control valley, the linear regression calculated from 1998 to 2017 showed a negative trend (β = −10.06; $R^2 = 0.16$; $p = 0.07965$). Though this trend was not significant, another regression including BAI values from 2009 to 2017 indicated similar trends but with a significant and more negative trend (β = –44.57; $R^2 = 0.53$; $p = 0.02643$).

3.2. C_i, $\Delta^{13}C$ and iWUE variations from 1959 to 2017

Intercellular CO_2 concentrations (C_i) increased significantly in the control valley ($p < 0.0001$) as well as in the treatment valley ($p < 0.0001$; Figure 6A). Despite a higher C_i in 1959 in the treatment valley (201 ppm) compared to the control valley (163 ppm), the overall increase in the control valley was faster than in the treatment valley and reached 238 ppm in 2017 (228 ppm in the treatment valley). Temporal change in $\Delta^{13}C$ presented opposite trends in the control and treatment valleys (Figure 6B). In the control valley, $\Delta^{13}C$ ranged from 16.6‰ (1959) to 18.9‰ (1979) before declining again to 17.6‰ (2017). The linear regression model showed that $\Delta^{13}C$ increased slightly over the 59 years tested. But the R^2 value was low and the linear regression model was not significant (y = 0.0033x + 10.688; $R^2 = 0.01$; $p > 0.05$). In the treatment valley, however, results from the linear regression showed a significant overall decrease of $\Delta^{13}C$ ($R^2 = 0.43$; $p < 0.0001$). However the R^2 was lower than 0.5 so this result should be taken with a grain of salt, since the model did not explain a majority of the variation in data.

A quadratic regression was used to represent the trends in iWUE (Figure 6C). The iWUE ranged from 75.25 μmol mol^{-1} to 118.02 μmol
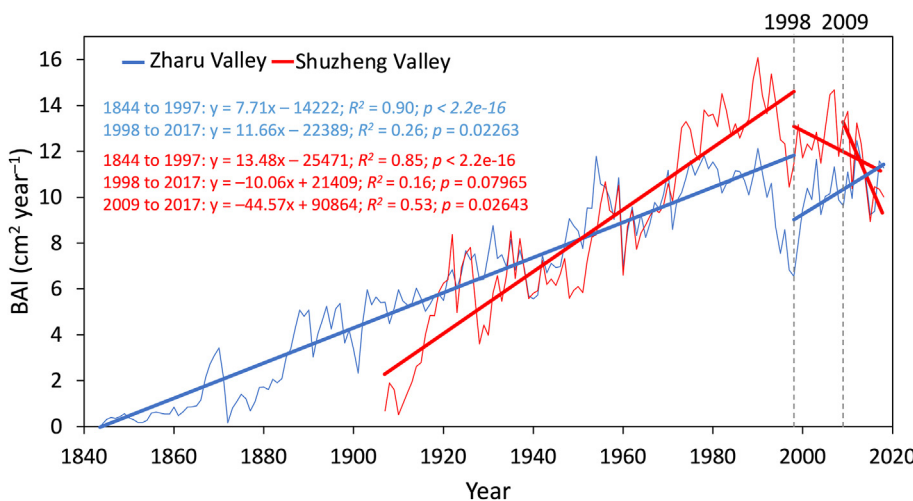

Figure 5. Averaged basal area increment (BAI) in Zharu Valley (control valley; n = 47 trees, blue line) and in Shuzheng Valley (treatment valley; n = 50 trees, red line). The dotted line at years 1998 and 2009 represent the beginning of rapid-growing tourism and very rapid-growing tourism in JNR, respectively. Blue bold lines show linear regressions from 1844 to 1997 and 1998 to 2017 in Zharu Valley. Red bold lines show linear regressions from 1944 to 1997, 1998 to 2017, and 2009 to 2017 in Shuzheng Valley. Equations and R^2 are noted for each linear regression.
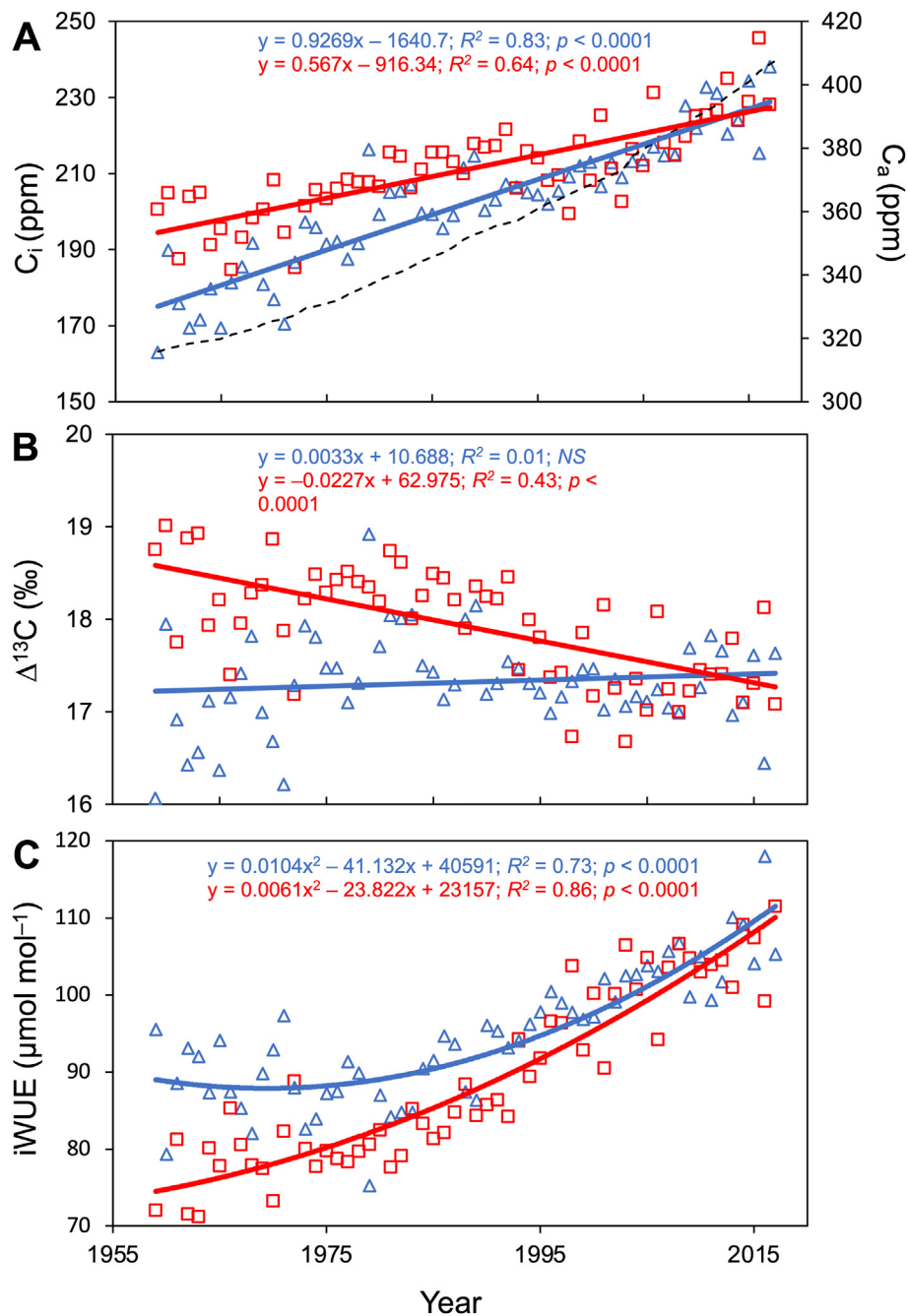
Figure 6. Annual changes in intercellular CO_2 concentration (C_i), carbon isotope discrimination ($\Delta^{13}C$), and intrinsic water-use efficiency (iWUE) from 1959 to 2017. C_i variation is presented in (**A**), $\Delta^{13}C$ in (**B**), and iWUE in (**C**). The black dotted line represents the ambient atmospheric CO_2 (C_a). Linear or quadratic regressions are represented by blue (control valley) and red (treatment valley) lines/curves.

mol^{-1} in the control valley and from 69.97 to 111.52 μmol mol^{-1} in the treatment valley between 1959 and 2017, exhibiting an increase of 25.3% and 47.8%, respectively (control valley $R^2 = 0.73$; $p < 0.0001$; treatment valley $R^2 = 0.86$; $p < 0.0001$). After the 1980s, iWUE increased faster in both valleys. Moreover, it is clear that C_i and iWUE increased in both control and treatment valleys, whereas the $\Delta^{13}C$ exhibited the opposite pattern, decreasing in the treatment valley and increasing in the control valley, though slightly.

3.3. Tree growth, C_i, and iWUE response to climate

Correlations between BAI and climate variables (e.g., mean monthly precipitation and mean monthly temperature) are shown in Figure 7. We found a significant correlation between precipitations and BAI in September of the previous year in the control valley ($r = 0.266$; $p < 0.05$; Figure 7A). Results from correlation analysis in the treatment valley did not show any significant correlation between precipitation and BAI (Figure 7C). The temperature in the control valley had a very weak link with BAI (Figure 7B). However, in the treatment valley, temperature in February ($r = 0.311$; $p < 0.05$) and in June ($r = 0.39$; $p < 0.05$) showed significant positive correlations with BAI (Figure 7D). The moving correlation analysis (Figures 8A and 8B) showed that the positive correlation in the treatment valley in June weakened over time (Figure 8B).

We found a very weak correlation between C_i and precipitation in the control valley ($R^2 = 0.04$; $p = 0.02$; Figure 9A). No correlation between precipitation and C_i was found in the treatment valley. In both valleys,
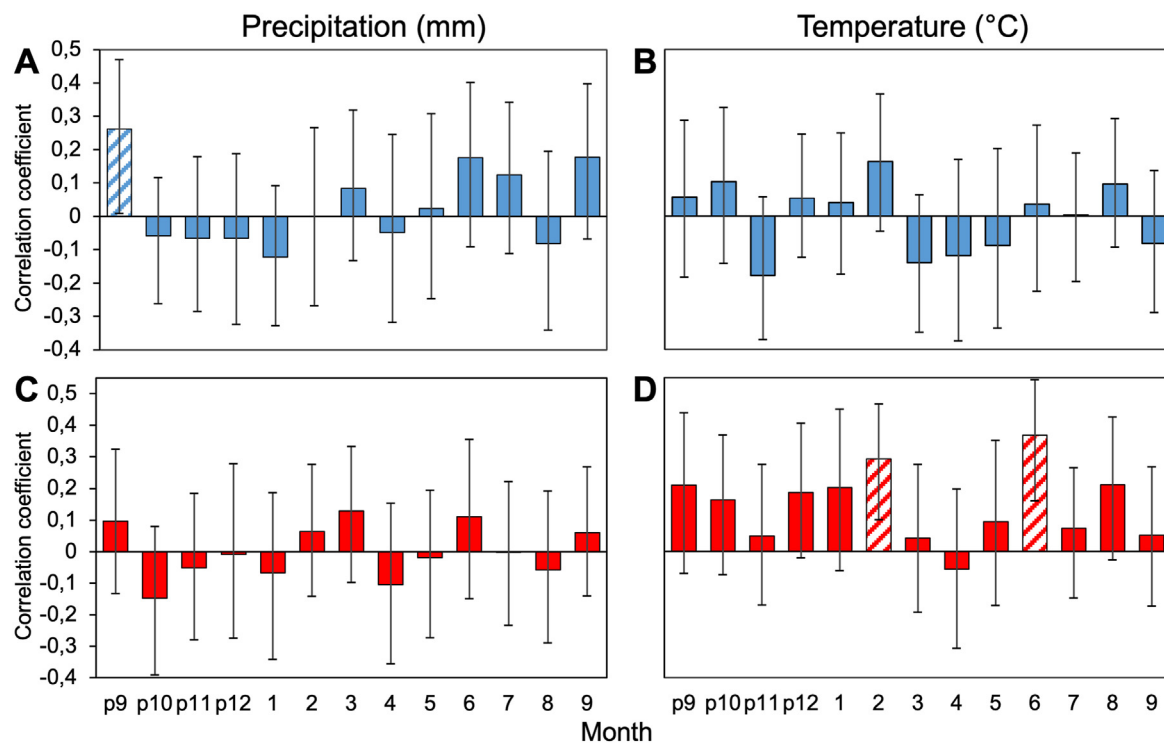
Figure 7. Correlation function between basal area increment (BAI) and climate variables in Zharu Valley and Shuzheng Valley (1951–2017). Zharu Valley (control valley) is shown in (**A**) and (**B**), blue bars. Shuzheng Valley (treatment valley) is shown is (**C**) and (**D**), red bars. Climate data were the monthly total precipitations and monthly average temperatures. The p followed by numbers in "Month" indicate months of the previous year. Significant levels are shown with hatch mark-colored bars (Package "bootRes" in R, bootstrap method, 1000 repetitions). Correlation coefficient is noted "*r*".

temperature exhibited by far the strongest influence on C_i, explaining about 41% of interannual variation in C_i in the control valley and 21% in the treatment valley. Regression analysis relating iWUE to changes in mean annual temperature showed significant positive relationships, with a stronger effect in the treatment valley (Figure 9B). Moreover, there was no relationship between iWUE and annual precipitation.

In addition, we represented three different gas exchange response scenarios to better understand tree physiological reactions to increasing atmospheric CO_2 concentrations (Saurer et al., 2004): (1) C_i remains constant and iWUE significantly increases; (2) C_i/C_a remains constant and iWUE slightly increases; (3) both C_a–C_i and iWUE remain constant. Results showed a significant increase of Ci in both valleys (Figures 10A and 10B). However, C_i/C_a was nearly constant ($\beta = 0.0002$) in the control valley while slightly decreasing in the treatment valley ($\beta = -0.001$) (Figures 10C and 10D). C_a–C_i increased in both valleys and increased more in the treatment valley (control: $\beta = 0.6085$, treatment: $\beta = 0.9817$) (Figures 10E and 10F).

3.4. Relationship between BAI and iWUE

The regression analysis did not show any relationship between iWUE and BAI in the control valley ($R^2 = 0.00003$; $p = 0.8991$; Figure 11A). For the treatment valley, a quadratic regression model showed a significant relationship between BAI and iWUE following a negative parabola shape ($R^2 = 0.33$; $p < 0.01$; Figure 11B). Furthermore, the correlation analysis between iWUE and C_a using a linear regression model indicated a strong positive correlation in the control valley ($R^2 = 0.67$; $p = 1.598e^{-15}$) and in the treatment Valley ($R^2 = 0.86$; $p < 2.2e^{-16}$; Figures 12A and 12B).

4. Discussion

4.1. Tree growth

In this study, we used BAI to characterize tree growth in a recently developed tourist destination with distinct development stages

characterized by different anthropogenic activities, number of tourists, and emissions. Since our sampling strategy avoided age-class bias (Cherubini et al., 1998; Brienen et al., 2012) and BAI calculation inherently removes the geometrical age trends without the need for detrending, age effect was minimized (although not completely excluded) by calculating BAI (Cherubini et al., 2021). BAI variation showed strong correlations between different altitudes (i.e., altitudinal transect design; Figure S5), BAI could be averaged for all trees within a valley to reveal different patterns in BAI variation in each of the two valleys with very different tourist impacts. The BAI trajectory fell within three main phases: (i) a steady increase from 1844 (control valley) and 1907 (treatment valley) to the early 1990s, (ii) a very fast decrease in BAI from the early to mid-1990s, and (iii) divergent BAI trends after 1998, either increasing (control valley) or decreasing (treatment valley). In phase (i), the BAI in the treatment valley increased faster than in the control valley, suggesting that the CFE was not as apparent in the control valley, probably due to its older trees, but the younger trees in the treatment valley appeared to benefit more from the CFE. This effect was also found in other studies (Fang et al., 2014; Abiyu et al., 2018) and could be explained in several ways. For example, less competition and better light and substrate resources in younger forests could result in higher growth rates (Brienen et al., 2012).

The decreasing BAI during phase (ii) could have been caused by a severe drought documented at that time. Thus, the CFE cannot compensate for the effects of increasing aridity on gas exchange, especially in forests with dry seasons (Barber et al., 2000; Peñuelas et al., 2008; Linares et al., 2009; Nock et al., 2011). The main divergence in BAI trends between the two valleys occurred in phase (iii) after 1998. Building on the example of the natural CO_2 springs studies (Hattenschwiler et al., 1997; Tognetti et al., 2000), this new research design showed different results. Our findings do clearly indicate that increasing atmospheric CO_2 (combined with optimal environmental conditions) did stimulate tree growth of Chinese pine on a centennial timescale in the control valley (and the treatment valley before the mid 1990s), but,
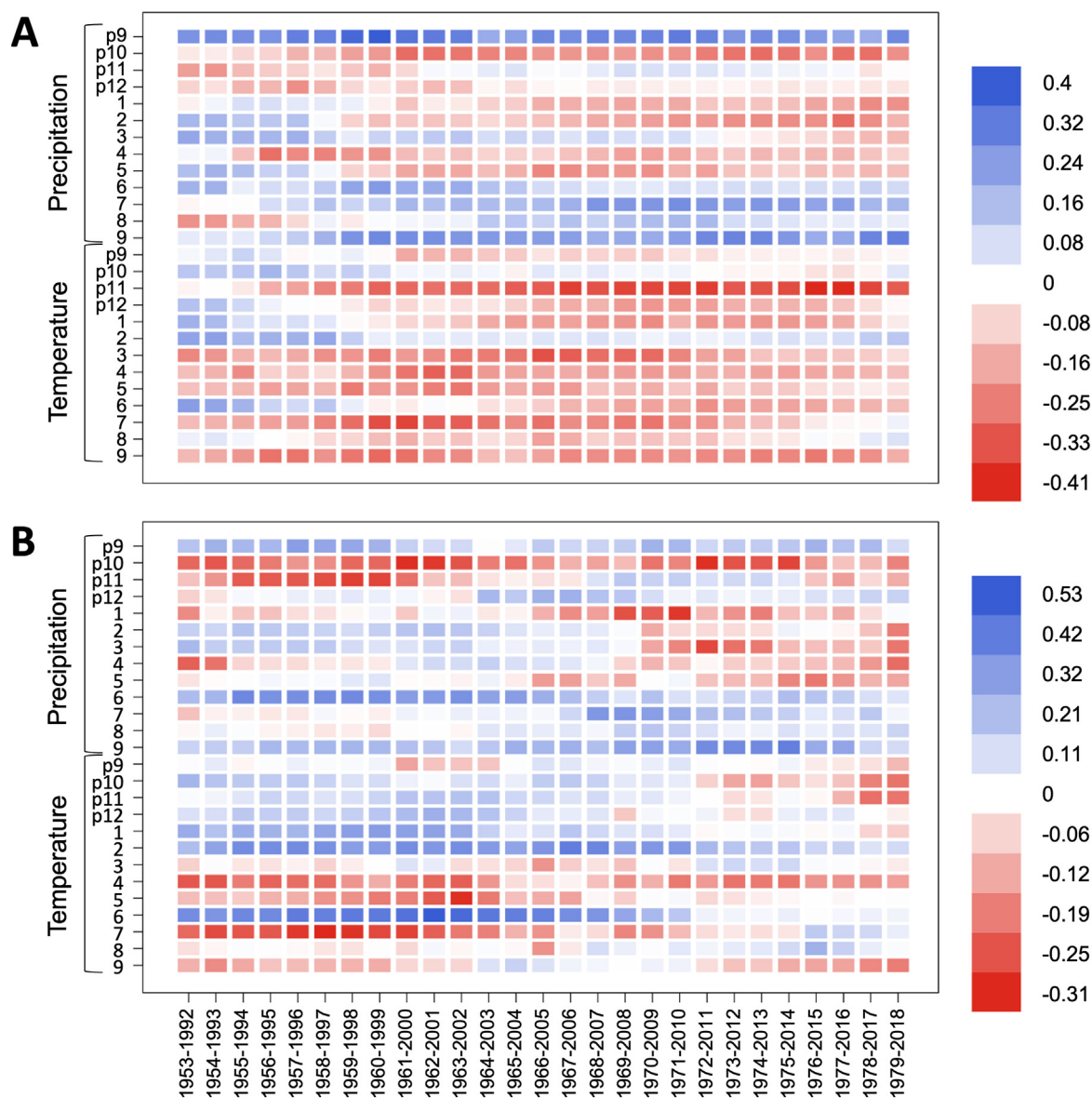
Figure 8. Moving correlation functions of temperature and precipitation for BAI in Zharu Valley (**A**, control valley) and Shuzheng Valley (**B**, treatment valley). The response function has been calculated from September (from previous year, noted "p9") to September (from current year, noted "9". The window size is 40 years, and the windows have been offset by one year. Positive response coefficients are shown by a blue gradient and negative response coefficients by a red gradient.

contrary to the common assumption, it did not stimulate tree growth under higher localized CO_2 concentrations in the treatment valley following the rapid increase in tourist visits. These results show that the CFE on long-term tree growth is likely to be overestimated under eCO_2 (Wang et al., 2020). Thus, more studies are needed to better assess carbon capture by forests in different biomes.

4.2. Is climate controlling BAI?

In the treatment valley, BAI and temperature significantly correlated in February and June. A study conducted on another conifer (*Picea likiangensis* var. *balfouriana*) not far from our site, also found a correlation between temperatures in June and BAI at high elevation (above 3500 m) (Wang et al., 2018). Since our study was not carried out at as high elevations (~2350 m), temperature may not be as an important factor controlling tree growth rate. By using moving correlation functions, we found that the positive correlation in the treatment valley in June weakened over time, especially following the 1972–2011 window. This could imply that increasing global temperatures (observed since the

1980s) has decreased the importance of seasonal changes in temperature on tree growth rate in Jiuzhaigou after that window. Also, increasing temperature together with decreasing precipitation likely led to drought (Figure S6), thereby inhibiting the CFE during the phase (ii) (Linares et al., 2009; Camarero et al., 2015; Reed et al., 2018; Maxwell et al., 2019).

4.3. Trends in iWUE: atmospheric CO_2 and climate contributions

In both valleys, we observed a significant, exponential increase in iWUE, consistent with other studies conducted over the past decade. In the control valley, iWUE rose by approximatively 25.3% from 1959 to 2017, and in the treatment valley the increase was even higher (47.8%). A recent study conducted in Jinchuan County in northwestern Sichuan Province, not far from JNR, showed that iWUE in *Picea likiangensis* var. *balfouriana* increased by 30.4% from 1851 to 2009 (Wang et al., 2018). Similarly, a study covering all major global forest biomes found an iWUE increase of 20.5% over the previous 40 years with no significant biome differences, although a slightly higher percentage change in iWUE
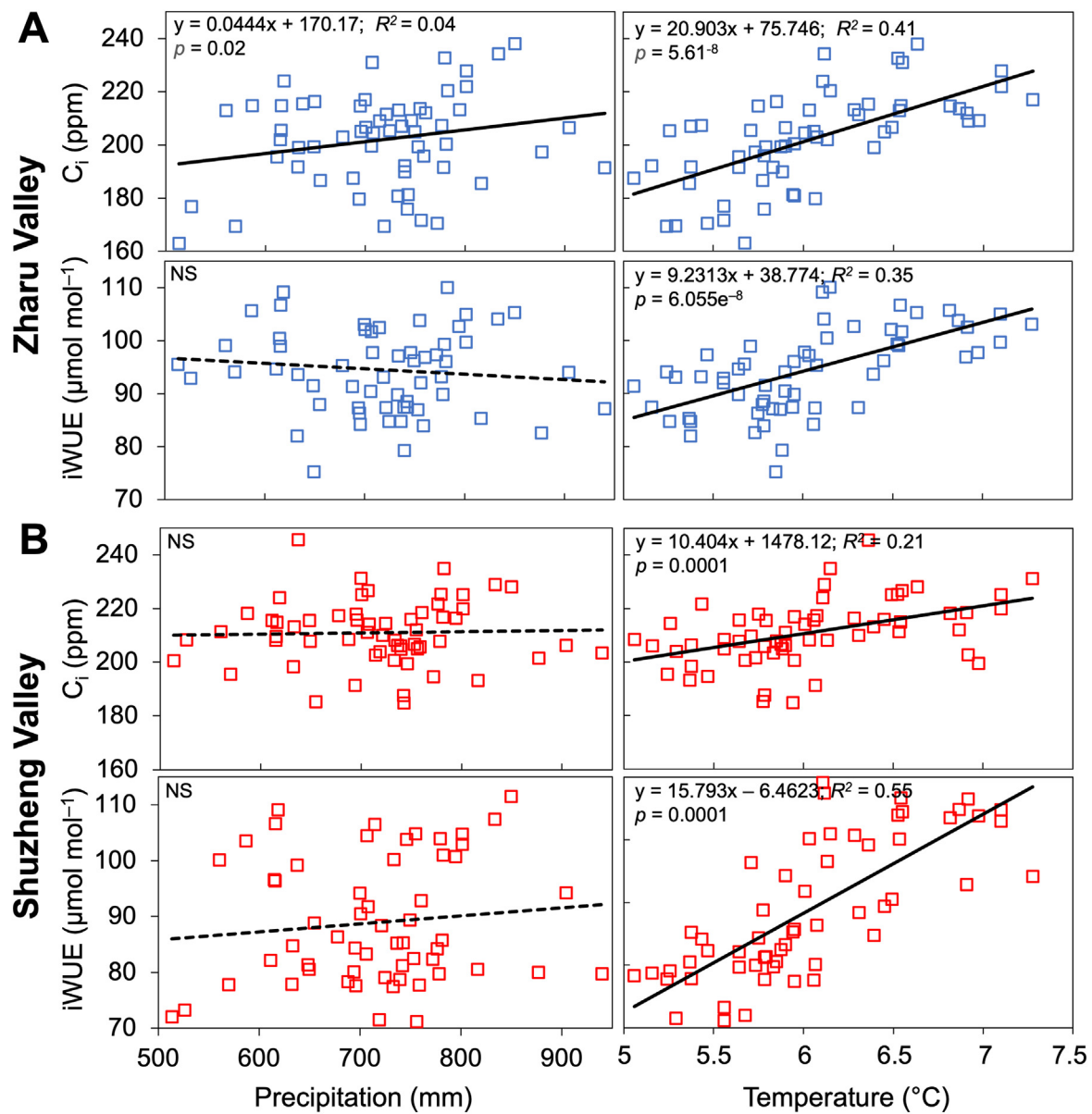
Figure 9. Intercellular CO_2 concentration (C_i) and intrinsic water-use efficiency (iWUE) vs. mean annual temperature and annual precipitation in Zharu Valley (control valley; **A**) and Shuzheng Valley (treatment valley; **B**) from 1959 to 2017. Significant regressions are indicated with solid black lines, while insignificant regressions are shown with dotted black lines. Climate data were taken from Songpan Weather Station.

occurred in temperate forests (Peñuelas et al., 2011). In a European temperate forest, a study found that iWUE increased approximately 22% (Frank et al., 2015). In Zharu Valley, which served as the control (e.g., ambient CO_2 concentrations), the increase in iWUE of 25.3% seems to be in line with increases documented elsewhere in temperate areas. Thus, our control valley exhibited similar increases to the global temperate forest average.

Interestingly, the iWUE increase in the treatment valley was nearly twice as high as that found in other studies. Several mechanisms could explain this significant increase. A long-term increase of iWUE indicates increasing net photosynthesis and/or decreasing stomatal conductance (and thus reduced transpiration). Because iWUE is expressed as the ratio of net photosynthesis to conductance for water vapor, it is very likely that the increase in atmospheric CO_2 concentration in the treatment valley has resulted in both increased photosynthesis and reduced transpiration (van der Sleen et al., 2014; Zuidema et al., 2020; Lauriks et al., 2021). The increase in temperatures observed since the 1980s (Figure S3) may indirectly result in higher iWUE as higher temperatures increase vapor

pressure deficits (VPD), to which trees may respond by closing their leaf stomata and therefore reducing g_w (Lloyd and Farquhar, 2008; Brienen et al., 2011). Thus, the exponential increase in iWUE beginning in the 1980s in both valleys confirms the importance of temperature in controlling iWUE. Future studies should consider calculating VPD, which could provide additional insight into variations in iWUE because of its importance in stomatal conductance variation and tree physiology (Lévesque et al., 2014).

The correlation analysis between iWUE and C_a using a linear regression model indicated a strong positive correlation in both control and treatment valleys (Figures 12A and 12B). These results also indicated iWUE in the treatment valley exhibited higher values than in the control valley for the same C_a values. C_a also seemed to play an important role in the iWUE trends, being likely that the increase in C_a was the main cause of the improved iWUE in both valleys. This makes sense because the theoretical equation used to calculate iWUE strongly depends on C_a (Ehleringer and Cerling, 1995; Saugier et al., 1993), so iWUE is significantly affected by CO_2 concentrations (Silva and Horwath, 2013).
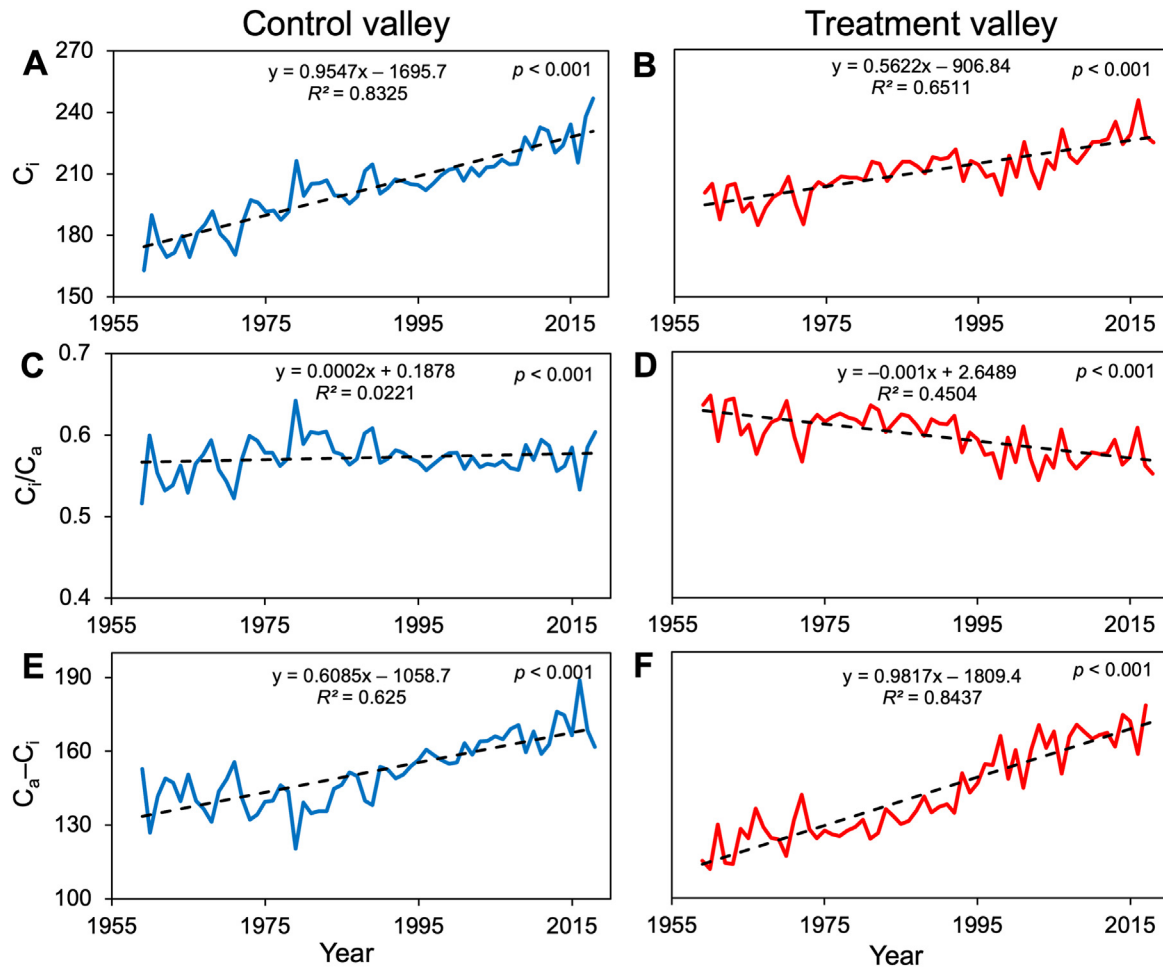
Figure 10. Trends in C_i, C_i/C_a, and C_a–C_i. **A, C, E** for the control (Zharu Valley) and **B, D, F** for the treatment (Shuzheng Valley) valleys. This figure is based on Saurer et al. (2004) three scenarios.
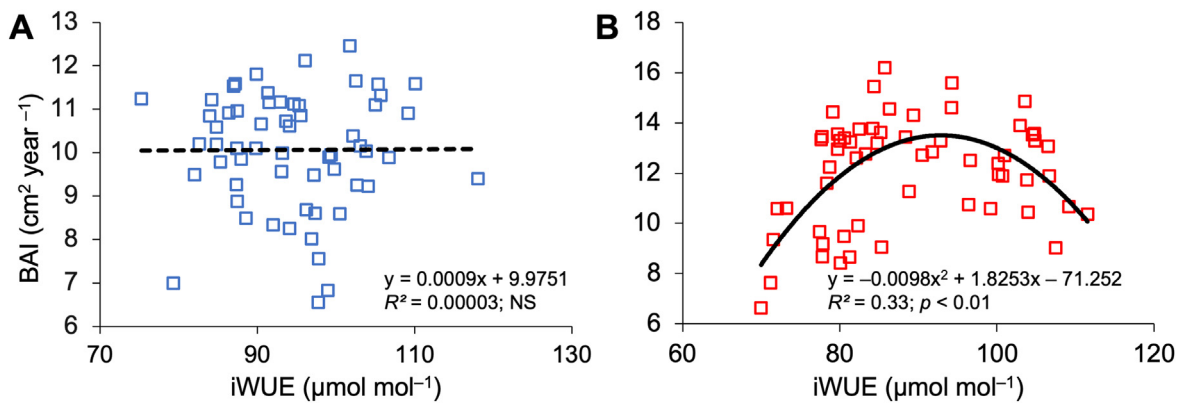

Figure 11. Relationship between basal area increment (BAI) and intrinsic water-use efficiency (iWUE) (**A**) in Zharu Valley (control valley, blue squares) and (**B**) in Shuzheng Valley (treatment valley, red squares). Data were used from the year 1959–2017. Regressions are indicated by a black line (significant) or a dotted line (insignificant). Equations of linear and quadratic regressions are shown for each graph.

Moreover, rising C_a limits leaf stomatal conductance but stimulates photosynthesis, thereby encouraging greater tree iWUE (Wang et al., 2018). This is in line with many other studies showing an improvement of iWUE under increasing CO_2 (Bert et al., 1997; Feng, 1999; Saurer et al., 2004; Waterhouse et al., 2004; Hietz et al., 2005; Brienen et al., 2011; Battipaglia et al., 2013; van der Sleen et al., 2014; Wang et al., 2018; Xu et al., 2018).

4.4. What does variation in C_i tell us?

In the control valley, the linear regression showed that despite the increase in C_i, the ratio C_i/C_a was constant and C_a–C_i showed a significant increasing trend (Figure 10). With respect to the three scenarios described by Saurer et al. (2004), these results correspond to scenario (2) which is the most common response inferred by tree rings (Feng, 1998;
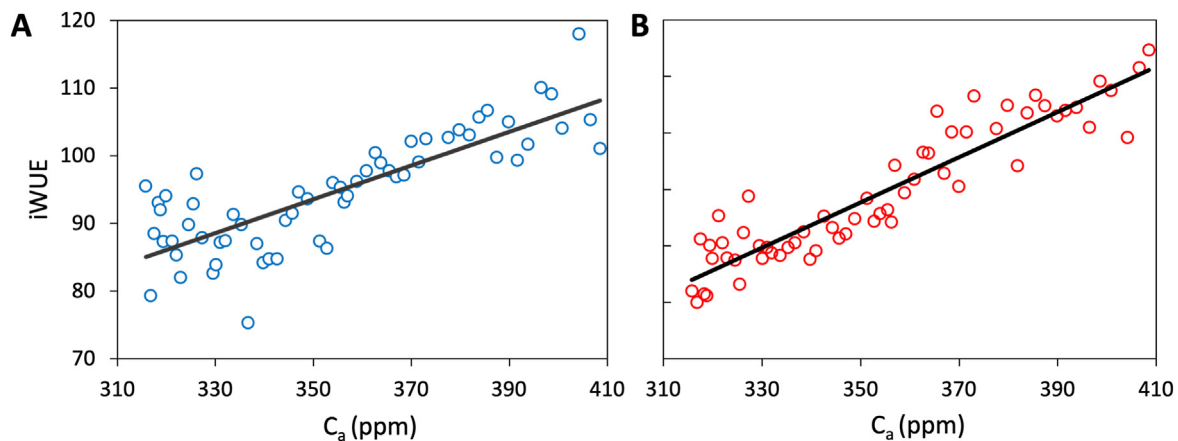
Figure 12. Correlation between atmospheric CO_2 (C_a) concentrations and iWUE in Zharu (**A**, control valley; blue circles) and Shuzheng (**B**, treatment valley; red circles). Linear regressions are represented by a black line. The equations of the linear regression are shown for each graph.

Saurer et al., 2004; Hietz et al., 2005; Nock et al., 2011). Constant C_i/C_a and an improvement in iWUE reflect proportional regulation of A and g_w. Also, it may indicate tree adaptation to C_a increases because of simultaneous decreases in both photosynthetic rate and stomatal conductance (Saurer et al., 2004; Andreu-Hayles et al., 2011; Brienen et al., 2011). In the treatment valley, C_i increased (slightly), the ratio C_i/C_a decreased, and C_a–C_i increased with improved iWUE, following scenario (1) (Saurer et al., 2004). These results indicate that other factors (e.g., eCO_2) are reinforcing the stomatal closure in the treatment valley. Other studies have reported similar results, exhibiting a decrease in $\Delta^{13}C$ associated with an improvement in iWUE (Peñuelas and Azcón-Bieto, 1992; Bert et al., 1997; Duquesnay et al., 1998; Hietz et al., 2005; Andreu-Hayles et al., 2011).

4.5. Relationship between iWUE and BAI

Our results showed no clear correlation between iWUE and BAI in the control valley, indicating the increasing BAI under ambient CO_2 levels were primarily attributed to increasing C_a, as climate variables did not significantly control tree growth variation. In the treatment valley, our results revealed that increasing localized eCO_2 led to an improvement in iWUE. Between 1959 and 1997, when iWUE was below 93 $\mu mol\ mol^{-1}$, the positive relationship between iWUE and BAI suggested that the increase in iWUE was driven by both increasing carboxylation and decreasing or constant g_w, under co-occurring and progressive warming and rising CO_2 concentrations. Meanwhile, the negative relationship between iWUE and BAI (for iWUE values higher than 93 $\mu mol\ mol^{-1}$, between 1998 and 2017) indicated that the iWUE increase was achieved primarily by decreased g_w which was not translated into improved tree growth. Similar results with a negative parabola shape were previously found in *Pinus densiflora*, indicating that temperature (and CO_2) rather than precipitation was an important factor controlling iWUE variation (Kwak et al., 2016).

The tree growth rate decline, with increasing temperature, particularly in the past three decades in the treatment valley, also suggests that increases in iWUE cannot compensate for the negative effects of severe water limitations on tree radial growth under eCO_2. An increase in iWUE with no apparent tree growth has been found in several other studies (Andreu-Hayles et al., 2011; Peñuelas et al., 2011; Gómez-Guerrero et al., 2013; Lévesque et al., 2014; Xu et al., 2018; Lu et al., 2019; Maxwell et al., 2019). Under eCO_2, it is also possible that the assimilated carbon was allocated more to the root development to facilitate water absorption from moisture-limited soils rather than to basal area growth. Some studies found that additional CO_2 assimilation does not result in stem

growth, thereby not detected in tree rings. Such allocation shifts might include increased seed production or investments in root biomass (Wright and Calderón, 2006; Iversen, 2010; van der Sleen et al., 2014).

4.6. Limitations of the study

The possible confounding effects of other pollutants emitted in JNR was not considered in this study. For example, SO_2 and NO_x emissions might also affect tree growth, so these pollutants could provide additional insight about stomatal conductance reduction in an area with eCO_2 concentrations (Choi and Lee, 2012). Thus, the role of other atmospheric air pollutants should be incorporated together with CO_2 in future studies to parse out their potential confounding effects on tree growth. Furthermore, we did not measure nitrogen and oxygen isotopes in this study. Further studies should utilize these isotopes to strengthen understanding of long-term nutrient and water limitation effects on tree growth under eCO_2.

5. Conclusion

This is the first study to simultaneously investigate the (1) long-term effects of (2) localized anthropogenic eCO_2 concentrations on (3) tree growth rate and (4) iWUE under (5) natural conditions. This novel approach brings new information concerning tree growth responses to eCO_2 concentrations with long-term tree growth records. Our results show that trees in the control site (Zharu Valley) may have benefited from increasing ambient C_a levels through the CFE. Although trees in the treatment site (Shuzheng Valley) also initially seemed to respond positively to the CFE, after being exposed to comparatively extreme levels of localized eCO_2, they experienced declines in tree radial growth. Despite a significant increase in iWUE in both valleys, iWUE likely did not benefit trees in the treatment valley because the eCO_2 and increasing temperature appear to have resulted in stomatal closure and a reduction of photosynthetic rates. Thus, the effect of increasing temperature and atmospheric CO_2 concentrations on terrestrial photosynthesis in the context of climate change on a global scale may be overestimated in current global warming models. That is, the potential for forests to "green the earth", mitigate CO_2, and reduce global warming may be more limited than predicted in dryer areas. This study provides data and useful insights to better manage natural areas, particularly in terms of developing ideal policies for managing heavy tourist flows. More studies aiming to find a CO_2 fertilization effect in natural areas with localized anthropogenic eCO_2 are needed in other biomes and utilizing different tree species.

Declarations

Data availability statement

Data will be made available on request.

Declaration of interest's statement

The authors declare no conflict of interest.

Additional information

Supplementary content related to this article has been published online at https://doi.org/10.1016/j.heliyon.2022.e11219.

References

Abiyu, A., Mokria, M., Gebrekirstos, A., Bräuning, A., 2018. Tree-ring record in Ethiopian church forests reveals successive generation differences in growth rates and disturbance events. For. Ecol. Manag. 409, 835–844.

Acock, B., Allen, L.H., 1985. Crop responses to elevated carbon dioxide concentrations. In: Strain, B.R., Cure, J.D. (Eds.), Direct Effects of Increasing Carbon Dioxide on Vegetation. (US Dept of Energy), pp. 53–97.

Ainsworth, E.A., Long, S.P., 2005. What have we learned from 15 years of Free-Air CO_2 Enrichment (FACE)? A meta-analytic review of the responses of photosynthesis, canopy properties and plant production to rising CO_2. New Phytol. 165, 351–372.

Allen, L.H., 1994. Carbon dioxide increase: direct impacts on crops and indirect effects mediated through anticipated climatic changes. In: Boote, K.J., Bennett, J.M., Sinclair, T.R., Paulsen, G.M. (Eds.), Physiology and Determination of Crop Yield. (American Society of Agronomy), pp. 425–459.

Allen, L.H., Amthor, J.S., 1995. Plant physiological responses to elevated CO_2, temperature, air pollution, and UV-B radiation. In: Woodwell, G.M., Mackenzie, F.T. (Eds.), Biotic Feedbacks in the Global Climatic System. Oxford University Press, pp. 51–84.

Allen, L.H., Valle, R.R., Mishoe, J.W., Jones, J.W., 1994. Soybean leaf gas-exchange responses to carbon dioxide and water stress. Agron. J. 86, 625–636.

Andreu-Hayles, L., Planells, O., Gutiérrez, E., Muntan, E., Helle, G., Anchukaitis, K.J., Schleser, G.H., 2011. Long tree-ring chronologies reveal 20th century increases in water-use efficiency but no enhancement of tree growth at five Iberian pine forests. Global Change Biol. 17, 2095–2112.

Bader, M.K.F., Leuzinger, S., Keel, S.G., Siegwolf, R.T.W., Hagedorn, F., Schleppi, P., Körner, C., 2013. Central european hardwood trees in a high-CO_2 future: synthesis of an 8-year forest canopy CO_2 enrichment project. J. Ecol. 101, 1509–1519.

Barber, V.A., Juday, G.P., Finney, B.P., 2000. Reduced growth of Alaskan white spruce in the twentieth century from temperature-induced drought stress. Nature 405, 668–673.

Bassett, J.R., 1964. Tree growth as affected by soil moisture availability. Soil Sci. Soc. Am. J. 28, 436–438.

Battipaglia, G., Saurer, M., Cherubini, P., Calfapietra, C., McCarthy, H.R., Norby, R.J., Francesca Cotrufo, M., 2013. Elevated CO_2 increases tree-level intrinsic water-use efficiency: insights from carbon and oxygen isotope analyses in Tree rings across three forest FACE sites. New Phytol. 197, 544–554.

Bert, D., Leavitt, S.W., Dupouey, J.-L., 1997. Variations of wood $\delta^{13}C$ and water-use efficiency of Abies alba during the last century. Ecology 78, 1588–1596.

Biondi, F., Waikul, K., 2004. DENDROCLIM2002: a C++ program for statistical calibration of climate signals in tree-ring chronologies. Comput. Geosci. 30, 303–311.

Biondi, F., Qeadan, F., 2008. A theory-driven approach to tree-ring standardization: defining the biological trend from expected basal area increment. Tree-Ring Res. 64, 81–96.

Bishop, K.A., Leakey, A.D., Ainsworth, E.A., 2014. How seasonal temperature or water inputs affect the relative response of C3 crops to elevated [CO2]: a global analysis of open top chamber and free Air CO2 enrichment studies. Food Energy Secur 3, 33–45.

Bonan, G.B., 2008. Forests and climate change: forcings, feedbacks, and the climate benefits of forests. Science 320, 1444–1449.

Brendel, O., Iannetta, P.P.M., Stewart, D., 2000. A rapid and simple method to isolate pure alpha-cellulose. Phytochem. Anal. 11, 7–10.

Brienen, R.J.W., Gloor, E., Zuidema, P.A., 2012. Detecting evidence for CO2 fertilization from tree ring studies: the potential role of sampling biases. Global Biogeochem. Cycles 26, GB1025.

Brienen, R.J.W., Wanek, W., Hietz, P., 2011. Stable carbon isotopes in tree rings indicate improved water-use efficiency and drought responses of a tropical dry forest tree species. Trees (Berl.) 25, 103–113.

Bunn, A.G., 2010. Statistical and visual crossdating in R using the DplR library. Dendrochronologia 28, 251–258.

Burk, R.L., Stuiver, M., 1981. Oxygen isotope ratios in trees reflect mean annual temperature and humidity. Science 211, 1417–1419.

Camarero, J.J., Gazol, A., Tardif, J.C., Conciatori, F., 2015. Attributing forest responses to global-change drivers: limited evidence of a CO2 fertilization effect in Iberian pine growth. J. Biogeogr. 42, 2220–2233.

Cherubini, P., Dobbertin, M., Innes, J.L., 1998. Potential sampling bias in long-term forest growth trends reconstructed from tree rings: a case study from the Italian Alps. For. Ecol. Manag. 109, 103–118.

Cherubini, P., Battipaglia, G., Innes, J.L., 2021. Tree vitality and forest health: can tree-ring stable isotopes Be used as indicators? Curr. Forestry Rep. 7, 69–80.

Choi, W., Lee, K., 2012. A short overview on linking annual tree ring carbon isotopes to historical changes in atmospheric environment. For. Sci. Technol. 8, 61–66.

Cure, J.D., Acock, B., 1986. Crop responses to carbon dioxide doubling: a literature survey. Agric. For. Meteorol. 38, 127–145.

D'Arrigo, R., Wilson, R., Liepert, B., Cherubini, P., 2008. On the 'divergence problem' in northern forests: a review of the tree-ring evidence and possible causes. Global Planet. Change 60, 289–305.

Dore, S., Hymus, G.J., Johnson, D.P., Hinkle, C.R., Valentini, R., Drake, B.G., 2003. Cross validation of open-top chamber and eddy covariance measurements of ecosystem CO2 exchange in a Florida scrub-oak ecosystem. Global Change Biol. 9, 84–95.

Drake, B.G., Leadley, P.W., Arp, W.J., Nassiry, D., Curtis, P.S., 1989. An open top chamber for field studies of elevated atmospheric CO2 concentration on saltmarsh vegetation. Funct. Ecol. 3, 363–371.

Du, J., Qiao, X., Zhang, M., Di, B., Tang, Y., 2018. Wetlands in the Jiuzhaigou world natural heritage site of south-west China: classification and recent changes. Mar. Freshw. Res. 69, 677–689.

Duquesnay, A., Bréda, N., Stievenard, M., Dupouey, J.-L., 1998. Changes of tree-ring δ13C and water-use efficiency of beech (Fagus sylvatica L.) in north-eastern France during the past century. Plant Cell Environ. 21, 565–572.

Ehleringer, J.R., Cerling, T.E., 1995. Atmospheric CO2 and the ratio of intercellular to ambient CO2 concentrations in plants. Tree Physiol. 15, 105–111.

Fang, J., Kato, T., Guo, Z., Yang, Y., Hu, H., Shen, H., Zhao, X., Kishimoto-Mo, A.W., Tang, Y., Houghton, R.A., 2014. Evidence for environmentally enhanced forest growth. Proc. Natl. Acad. Sci. USA 111, 9527–9532.

Farquhar, G.D., Ehleringer, J.R., Hubick, K.T., 1989. Carbon isotope discrimination and photosynthesis. Annu. Rev. Plant Physiol. Plant Mol. Biol. 40, 503–537.

Feng, X., 1999. Trends in Intrinsic Water-use efficiency of natural trees for the past 100–200 years: a response to atmospheric CO_2 concentration. Geochem. Cosmochim. Acta 63, 1891–1903.

Feng, X., 1998. Long-term Ci/Ca response of trees in western north America to atmospheric CO2 concentration derived from carbon isotope chronologies. Oecologia 117, 19–25.

Frank, D.C., Poulter, B., Saurer, M., Esper, J., Huntingford, C., Helle, G., Treydte, K., Zimmermann, N.E., Schleser, G.H., Ahlström, A., 2015. Water-use efficiency and transpiration across European forests during the Anthropocene. Nat. Clim. Change 5, 579–583.

Fritts, H.C., 1976. Tree Rings and Climate. Academic Press London.

Gagen, M., Finsinger, W., Wagner-Cremer, F., McCarroll, D., Loader, N.J., Robertson, I., Jalkanen, R., Young, G., Kirchhefer, A., 2011. Evidence of changing intrinsic water-use efficiency under rising atmospheric CO2 concentrations in boreal Fennoscandia from subfossil leaves and tree ring $\Delta^{13}C$ ratios. Global Change Biol. 17, 1064–1072.

Gedalof, Z., Berg, A.A., 2010. Tree ring evidence for limited direct CO2 fertilization of forests over the 20th century: limited CO2 fertilization of forests. Global Biogeochem. Cycles 24, GB3027.

Girardin, M.P., Bernier, P.Y., Raulier, F., Tardif, J.C., Conciatori, F., Guo, X.J., 2011. Testing for a CO_2 fertilization effect on growth of Canadian boreal forests. J. Geophys. Res. 116, G01012.

Girardin, M.P., Bouriaud, O., Hogg, E.H., Kurz, W., Zimmermann, N.E., Metsaranta, J.M., de Jong, R., Frank, D.C., Esper, J., Büntgen, U., et al., 2016. No growth stimulation of Canada's boreal forest under half-century of combined warming and CO_2 fertilization. Proc. Natl. Acad. Sci. U.S.A. 113, E8406–E8414.

Gómez-Guerrero, A., Silva, L.C., Barrera-Reyes, M., Kishchuk, B., Velázquez-Martínez, A., Martínez-Trinidad, T., Plascencia-Escalante, F.O., Horwath, W.R., 2013. Growth decline and divergent tree ring isotopic composition ($\delta^{13}C$ and $\delta^{18}O$) contradict predictions of $CO2$ stimulation in high altitudinal forests. Global Change Biol. 19, 1748–1758.

Grant, R.F., Kimball, B.A., Pinter, P.J., Wall, G.W., Garcia, R.L., La Morte, R.L., Hunsaker, D.J., 1995. Carbon Dioxide effects on crop energy balance: testing ecosys with a Free-Air CO_2 Enrichment (FACE) experiment. Agron. J. 87, 446–457.

Guerrieri, R., Belmecheri, S., Ollinger, S.V., Asbjornsen, H., Jennings, K., Xiao, J., Stocker, B.D., Martin, M., Hollinger, D.Y., Bracho-Garrillo, R., et al., 2019. Disentangling the role of photosynthesis and stomatal conductance on rising forest water-use efficiency. Proc. Natl. Acad. Sci. U.S.A. 116, 16909–16914.

Hattenschwiler, S., Miglietta, F., Raschi, A., Korner, C., 1997. Thirty years of in situ tree growth under elevated CO_2: a model for future forest responses? Global Change Biol. 3, 463–471.

Hayhoe, K., Edmonds, J., Kopp, R., LeGrande, A., Sanderson, B., Wehner, M., Wuebbles, D., 2017. Climate Science Special Report: A Sustained Assessment Activity of the U.S. In: Wuebbles, D.J., Fahey, D.W., Hibbard, K.A., Dokken, D.J., Stewart, B.C., Maycock, T.K. (Eds.), Global Change Research Program: Washington), pp. 186–227.

Hendrey, G.R., Lewin, K.F., Nagy, J., 1993. Free air carbon dioxide enrichment: development, progress, results. Vegetatio 104, 17–31.

Hepburn, C., Adlen, E., Beddington, J., Carter, E.A., Fuss, S., Mac Dowell, N., Minx, J.C., Smith, P., Williams, C.K., 2019. The technological and economic prospects for CO_2 utilization and removal. Nature 575, 87–97.

Hietz, P., Wanek, W., Dünisch, O., 2005. Long-term trends in cellulose $\delta^{13}C$ and water-use efficiency of tropical Cedrela and Swietenia from Brazil. Tree Physiol. 25, 745–752.

Huntingford, C., Oliver, R.J., 2021. Constraints on estimating the CO_2 fertilization effect emerge. Nature 600, 224–225.

Iversen, C.M., 2010. Digging deeper: fine-root responses to rising atmospheric CO_2 concentration in forested ecosystems. New Phytol. 186, 346–357.

Jones, A.G., Scullion, J., Ostle, N., Levy, P.E., Gwynn-Jones, D., 2014. Completing the FACE of elevated CO_2 research. Environ. Int. 73, 252–258.

Kimball, B.A., 1983. Carbon dioxide and agricultural yield: an assemblage and analysis of 430 prior observations. Agron. J. 75, 779–788.

Kwak, J.-H., Lim, S.-S., Lee, K.-S., Viet, H.D., Matsushima, M., Lee, K.-H., Jung, K., Kim, H.-Y., Lee, S.-M., Chang, S.X., et al., 2016. Temperature and air pollution affected tree ring $\delta^{13}C$ and water-use efficiency of pine and oak trees under rising CO_2 in a humid temperate forest. Chem. Geol. 420, 127–138.

Lauriks, F., Salómon, R.L., Steppe, K., 2021. Temporal variability in tree responses to elevated atmospheric CO_2. Plant Cell Environ. 44, 1292–1310.

Lévesque, M., Siegwolf, R., Saurer, M., Eilmann, B., Rigling, A., 2014. Increased water-use efficiency does not lead to enhanced tree growth under xeric and mesic conditions. New Phytol. 203, 94–109.

Lewis, S.L., Wheeler, C.E., Mitchard, E.T.A., Koch, A., 2019. Restoring natural forests is the best way to remove atmospheric carbon. Nature 568, 25–28.

Li, D., Fang, K., Li, Yingjun, Chen, D., Liu, X., Dong, Z., Zhou, F., Guo, G., Shi, F., Xu, C., et al., 2017. Climate, intrinsic water-use efficiency and tree growth over the past 150 years in humid subtropical China. PLoS One 12, e0172045.

Linares, J.-C., Delgado-Huertas, A., Camarero, J.J., Merino, J., Carreira, J.A., 2009. Competition and drought limit the response of water-use efficiency to rising atmospheric carbon dioxide in the Mediterranean fir *Abies pinsapo*. Oecologia 161, 611–624.

Liu, S.Y., Zhang, X.P., Zeng, Z.Y., 2007. Biodiversity of the Jiuzhaigou National Nature reserve (In Chinese). Sichuan Science and Technology Publishing House, Chengdu, PR China.

Lloyd, J., Farquhar, G.D., 2008. Effects of rising temperatures and [CO_2] on the physiology of tropical forest trees. Philos. Trans. R. Soc. B: Biol. Sci. 363, 1811–1817.

Lu, K., Chen, N., Zhang, X., Wang, J., Wang, M., Khan, S., Han, C., Zhang, C., Wang, S., Wang, L., et al., 2019. Increased drought and atmospheric CO_2 positively impact intrinsic water-use efficiency but do not promote tree growth in semi-arid areas of northwestern China. Trees (Berl.) 33, 669–679.

Marshall, J.D., Monserud, R.A., 1996. Homeostatic gas-exchange parameters inferred from $^{12}C/^{13}C$ in tree rings of conifers. Oecologia 105, 13–21.

Maxwell, J.T., Harley, G.L., Mandra, T.E., Yi, K., Kannenberg, S.A., Au, T.F., Robeson, S.M., Pederson, N., Sauer, P.E., Novick, K.A., 2019. Higher CO_2 concentrations and lower cidic deposition have not changed drought response in tree growth but do influence iWUE in hardwood trees in the midwestern United States. J. Geophys. Res. Biogeosci. 124, 3798–3813.

Mazany, T., Lerman, J.C., Long, A., 1980. Carbon-13 in tree-ring cellulose as an indicator of past climates. Nature 287, 432–435.

McCarroll, D., Loader, N.J., 2004. Stable isotopes in tree rings. Quat. Sci. Rev. 23, 771–801.

MieliKainen, K., Timonen, M., 1996. Growth trends of Scots pine (*Pinus sylvestris* L.) in unmanaged and regularly managed stands in southern and central Finland. In: Spiecker, H., Mielikäinen, K., Köhl, M., Skovsgaard, J.P. (Eds.), Growth Trends in European Forests. Springer, pp. 41–59.

Nock, C.A., Baker, P.J., Wanek, W., Leis, A., Grabner, M., Bunyavejchewin, S., Hietz, P., 2011. Long-term increases in intrinsic water-use efficiency do not lead to increased stem growth in a tropical monsoon forest in western Thailand. Global Change Biol. 17, 1049–1063.

Norby, R.J., Zak, D.R., 2011. Ecological lessons from free-air CO_2 enrichment (FACE) experiments. Annu. Rev. Ecol. Evol. Syst. 42, 181–203.

Nordhaus, W., 2018. Projections and uncertainties about climate change in an era of minimal climate policies. Am. Econ. J. Econ. Pol. 10, 333–360.

Osmond, C.B., Björkman, O., Anderson, D.J., 1980. Physiological Processes in Plant Ecology: toward a Synthesis with atriplex. Springer Science & Business Media.

Peñuelas, J., Azcón-Bieto, J., 1992. Changes in leaf $\Delta^{13}C$ of herbarium plant species during the last 3 centuries of CO_2 increase. Plant Cell Environ. 15, 485–489.

Peñuelas, J., Canadell, J.G., Ogaya, R., 2011. Increased water-use efficiency during the 20th century did not translate into enhanced tree growth. Global Ecol. Biogeogr. 20, 597–608.

Peñuelas, J., Hunt, J.M., Ogaya, R., Jump, A.S., 2008. Twentieth century changes of tree-ring $\delta 13C$ at the southern range-edge of Fagus sylvatica: increasing water-use efficiency does not avoid the growth decline induced by warming at low altitudes. Global Change Biol. 14, 1076–1088.

Qiao, X., Du, J., Kota, S.H., Ying, Q., Xiao, W., Tang, Y., 2018. Wet deposition of sulfur and nitrogen in Jiuzhaigou National Nature Reserve, Sichuan, China during 2015-2016: possible effects from regional emission reduction and local tourist activities. Environ. Pollut. 233, 267–277.

Rahman, M., Islam, M., Gebrekirstos, A., Bräuning, A., 2019. Trends in tree growth and intrinsic water-use efficiency in the tropics under elevated CO_2 and climate change. Trees (Berl.) 33, 623–640.

Reed, C.C., Ballantyne, A.P., Cooper, L.A., Sala, A., 2018. Limited evidence for CO_2-related growth enhancement in northern Rocky Mountain lodgepole pine populations across climate gradients. Global Change Biol. 24, 3922–3937.

Rinn, F., 2003. TSAP-win. Time Series Analysis and Presentation for Dendrochronology and 409 Related Applications. User Reference.

Rozema, J., 1993. Plant responses to atmospheric carbon dioxide enrichment: interactions with some soil and atmospheric conditions. Vegetatio 104, 173–192.

Rubino, D.L., McCarthyz, B.C., 2004. Comparative analysis of dendroecological methods used to assess disturbance events. Dendrochronologia 21, 97–115.

Saugier, B., Ehleringer, J.R., Hall, A.E., Farquhar, G.D., 1993. Stable Isotopes and Plant Carbon-Water Relations, first ed. Academic Press.

Saurer, M., Siegwolf, R.T.W., Schweingruber, F.H., 2004. Carbon isotope discrimination indicates improving water-use efficiency of trees in northern Eurasia over the last 100 years. Global Change Biol. 10, 2109–2120.

Saurer, M., Spahni, R., Frank, D.C., Joos, F., Leuenberger, M., Loader, N.J., McCarroll, D., Gagen, M., Poulter, B., Siegwolf, R.T., 2014. Spatial variability and temporal trends in water-use efficiency of European forests. Global Change Biol. 20, 3700–3712.

Schweingruber, F.H., Briffa, K.R., Nogler, P., 1993. A tree-ring densitometric transect from Alaska to Labrador. Int. J. Biometeorol. 37, 151–169.

Silva, L., Horwath, W.R., 2013. Explaining global increases in water use efficiency: why have we overestimated responses to rising atmospheric CO_2 in natural forest ecosystems? PLoS One 8, e53089.

Silva, L.C.R., Anand, M., 2013. Probing for the influence of atmospheric CO_2 and climate change on forest ecosystems across biomes: changes in growth and iWUE across biomes. Global Ecol. Biogeogr. 22, 83–92.

Silva, L.C.R., Anand, M., Leithead, M.D., 2010. Recent widespread tree growth decline despite increasing atmospheric CO_2. PLoS One 5, e11543.

Tognetti, R., Cherubini, P., Innes, J.L., 2000. Comparative stem-growth rates of Mediterranean trees under background and naturally enhanced ambient CO_2 concentrations. New Phytol. 146, 59–74.

Tognetti, R., Lombardi, F., Lasserre, B., Cherubini, P., Marchetti, M., 2014. Tree-ring stable isotopes reveal twentieth-century increases in water-use efficiency of *Fagus sylvatica* and *Nothofagus* spp. in Italian and Chilean mountains. PLoS One 9, e113136.

van der Sleen, P., Groenendijk, P., Vlam, M., Anten, N.P.R., Boom, A., Bongers, F., Pons, T.L., Terburg, G., Zuidema, P.A., 2014. No growth stimulation of tropical trees by 150 years of CO_2 fertilization but water-use efficiency increased. Nat. Geosci. 8, 24–28.

Veihmeyer, F.J., Hendrickson, A.H., 1950. Soil moisture in relation to plant growth. Annu. Rev. Plant Physiol. 1, 285–304.

Walker, A.P., Kauwe, M.G.D., Bastos, A., Belmecheri, S., Georgiou, K., Keeling, R.F., McMahon, S.M., Medlyn, B.E., Moore, D.J.P., Norby, R.J., et al., 2021. Integrating the evidence for a terrestrial carbon sink caused by increasing atmospheric CO_2. New Phytol. 229, 2413–2445.

Wang, G.G., Chhin, S., Bauerle, W.L., 2006. Effect of natural atmospheric CO_2 fertilization suggested by open-grown white spruce in a dry environment. Global Change Biol. 12, 601–610.

Wang, J.-W., Denning, A.S., Lu, L., Baker, I.T., Corbin, K.D., Davis, K.J., 2007. Observations and simulations of synoptic, regional, and local variations in atmospheric CO_2. J. Geophys. Res. Atmos. 112, D04108.

Wang, S., Zhang, Y., Ju, W., Chen, J.M., Ciais, P., Cescatti, A., Sardans, J., Janssens, I.A., Wu, M., Berry, J.A., et al., 2020. Recent global decline of CO_2 fertilization effects on vegetation photosynthesis. Science 370, 1295–1300.

Wang, Y., Zhang, Y., Fang, O., Shao, X., 2018. Long-term changes in the tree radial growth and intrinsic water-use efficiency of Chuanxi spruce (*Picea likiangensis* var. balfouriana) in southwestern China. J. Geogr. Sci. 28, 833–844.

Waterhouse, J.S., Switsur, V.R., Barker, A.C., Carter, A.H.C., Hemming, D.L., Loader, N.J., Robertson, I., 2004. Northern European trees show a progressively diminishing response to increasing atmospheric carbon dioxide concentrations. Quat. Sci. Rev. 23, 803–810.

Way, D.A., Cook, A., Rogers, A., 2021. The effects of rising CO_2 concentrations on terrestrial systems: scaling it up. New Phytol. 229, 2383–2385.

Websites: US Department of Commerce, 2019. Global Monitoring Laboratory - Carbon Cycle Greenhouse Gases. https://www.esrl.noaa.gov/gmd/ccgg/trends/.

West, P.W., 1980. Use of diameter increment and basal area increment in tree growth studies. Can. J. For. Res. 10, 71–77.

Wigley, T.M., Briffa, K.R., Jones, P.D., 1984. On the average value of correlated time series, with applications in dendroclimatology and hydrometeorology. J. Appl. Meteorol. Climatol. 23, 201–213.

Wilson, A.T., Grinsted, M.J., 1977. ^{12}C/^{13}C in cellulose and lignin as palaeothermometers. Nature 265, 133–135.

Wright, S.J., Calderón, O., 2006. Seasonal, El Nino and longer term changes in flower and seed production in a moist tropical forest. Ecol. Lett. 9, 35–44.

Xu, G., Liu, X., Belmecheri, S., Chen, T., Wu, G., Wang, B., Zeng, X., Wang, W., 2018. Disentangling contributions of CO_2 concentration and climate to changes in intrinsic water-use efficiency in the arid boreal forest in China's Altay Mountains. Forests 9, 642.

Zang, C., Biondi, F., 2013. Dendroclimatic calibration in R: the BootRes package for response and correlation function analysis. Dendrochronologia 31, 68–74.

Zhang, M., Seyler, B.C., Di, B., Wang, Y., Tang, Y., 2021. Impact of earthquakes on natural area-driven tourism: case study of China's Jiuzhaigou National Scenic Spot. Int. J. Disaster Risk Reduc. 58, 102216.

Zhu, Z., Piao, S., Myneni, R.B., Huang, M., Zeng, Z., Canadell, J.G., Ciais, P., Sitch, S., Friedlingstein, P., Arneth, A., et al., 2016. Greening of the earth and its drivers. Nat. Clim. Change 6, 791–795.

Zuidema, P.A., Heinrich, I., Rahman, M., Vlam, M., Zwartsenberg, S.A., van der Sleen, P., 2020. Recent CO_2 rise has modified the sensitivity of tropical tree growth to rainfall and temperature Glob. Change Biol 26, 4028–4041.